

# Assessment of Direct Microrobotic Gripping for Single Flax Fibre Tensile Tests

Anouk Chevallier<sup>1</sup>, Ali Zarei<sup>2</sup>, Olli Tanhuanpää<sup>3</sup>, Markus Kakkonen<sup>3</sup>, Lassi Sukki<sup>2</sup>, Florian Boutenel<sup>1</sup>, Violaine Guicheret<sup>1</sup>, Vincent Placet<sup>1</sup>, Pasi Kallio<sup>2</sup> and Cédric Clévy<sup>1</sup>

**Abstract**—This paper deals with first investigations of a disruptive approach to achieve tensile tests of single plant fibres based on direct microrobotic gripping. Usually these tests are carried out by mechanical clamping jaws or using sample holder with adhesive. This new approach intends to bring versatility, automation and the capability to test fibres of much smaller length which is expected to avoid strong statistical bias induced by limitations of current approaches. A microrobotic experimental platform has been developed and two grippers with different gripping jaws are designed to address the important issue of clamping/boundary conditions. Experimental investigations were conducted on 20 tensile tests, validating the viability of the approach. Young’s modulus and stress at failure were identified and are in good correspondence with results available in the recent literature of flax fibres. This microrobotics approach is applicable for much smaller fibres, in a faster way and paves the way for large series of experiments possible through future automation.

## I. INTRODUCTION

Bio-based composites reinforced with annual plant fibres such as flax offer a reduced environmental footprint compared to composites incorporating synthetic fibres [1], [2], [3]. Faced with the need to predict the mechanical performance of these bio-based composites, it is essential to characterise the fibres composing them, particularly in terms of tensile properties. Compared to synthetic fibres, single plant fibres have several specificities of key importance including a complex morphology (Figure 1) and a heterogeneous multilayer microstructure. Their mechanical properties, highly anisotropic, are also linked to their biochemical composition [1], [4]. Thus, the interest in carrying out mechanical characterisation tests at the single fibre level increased recently. Nevertheless, single flax fibres are also very small (typically diameter in the order of 20  $\mu\text{m}$ ) making such tests particularly challenging [5], [6].

Longitudinal Young’s modulus ( $E_L$ ) and stress at failure ( $\sigma_f$ ) are two crucial parameters required in the design of bio-based composites parts for structural applications. Tensile tests aim to identify them.

A tensile test on a single plant fibre consists in positioning a fibre between two jaws. A tensile force of the order of a hundred milliNewtons is then applied, along with a displace-

ment of no more than a few tens of micrometres. Throughout the test, both force and displacement are measured.

Several works have already investigated experimental measurements based on single plant fibre tensile tests. The methods used are mainly of two types. A first one is based on mechanical principles at a reduced scale of jaws where the fibre is clamped. This principle enables a direct clamping of the fibre but, at this scale, alignments appear complex as well as the control of the clamping (boundary conditions of the problem) [7]. The second one is based on the use of adhesive with a paper frame, a sample holder [8] or glue droplets [9] that facilitates the clamping of the fibre and alignments. But, this leads to additional sources of uncertainty, particularly concerning the adhesion between glue and fibres or the introduction of glue into the fibres thus modifying the tested object. Both principles, despite their advantages and drawbacks, make it possible to identify Young’s modulus and stress at failure, but they require a complex procedure to prepare the fibre in order to successfully carry out the test. Because of the fibre size, hand manipulation used for this preparation step is particularly difficult. A solution consists in attaching one fibre by hand to a paper frame and installing it inside the tensile test machine. This preparation step appears complex, time consuming, introduces many angular parameters but also strong statistical biases [8]. These frames are also designed to facilitate manual tasks and are therefore centimetre-sized. The selected fibres are at least one centimetre long, inducing severe potential statistical biases as only the most mechanically robust and longest fibres are tested [10].

Moreover, the characteristics of flax fibres, as well as the various growth conditions they can experience, contribute to the variability in morphology and mechanical properties observed in the tested single plant fibres [11]. To obtain a statistical representation of this variability, it is essential to carry out a significant number of tests, ideally several hundreds [12]. Furthermore, it is substantial to enable tests on a wider variety of fibres, more especially fibres having a length of few millimetres [13], [14]. Consequently, automating the whole process, i.e. more especially the fibre preparation before testing and carrying out the tests is essential.

To address this key lock, a game changing approach is proposed based on microrobotics because it has already demonstrated very promising potential in terms of positioning control [15], [16] including when using microgrippers [17], [18], [19]. The proposed approach is especially based on microrobotics and microgrippers used as clamping jaws.

<sup>1</sup>Université de Franche-Comté, SUPMICROTECH-ENSMM, CNRS, FEMTO-ST Institute, 25000 Besançon, France  
anouk.chevallier@femto-st.fr, cedric.clevy@femto-st.fr

<sup>2</sup>Faculty of Medicine and Health Technology, Tampere University, Finland  
pasi.kallio@tuni.fi

<sup>3</sup>Fibrobotics Oy, Korkeakoulunkatu 1, 33720 Tampere, Finland

This approach offers numerous advantages including a high potential to automate the whole process, the capability to consider all fibres regardless of their morphology and size, preventing from complex handmade test preparation, setting alignments and angles by robot motions in order to reduce statistical biases. In addition, microgrippers enable a direct gripping of the fibres which also simplifies the data processing to identify the mechanical parameters. Grippers have already been used to study the bond strength of pulp fibres to each other [20] but the force magnitude was not as high as in a tensile test.

This paper thus aims at studying the potential of the microrobotic approach in tensile testing of flax fibres. For that, an experimental set-up has been developed and is introduced in Section II A. First tests shown that boundary conditions of the fibres during such tests are difficult to control when using gripper fingers with a flat surface in contact with the fibre of which results in sliding for all the tests. To address this important issue, Section II A introduces the design of two specific finger grippers (named Crocodile Gripper (CG) and Wave Gripper (WG)). Section II B then presents the conditions for testing and obtaining the mechanical properties. Section III showcases experimental results carried out using these two kinds of grippers and the related Young's modulus and stress at failure identified for flax fibres. Section IV gives concluding remarks and discussions of the work.

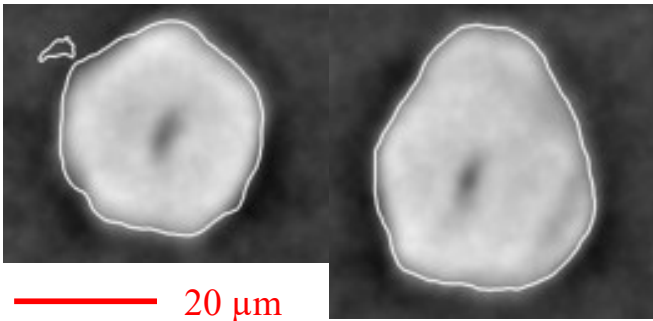


Fig. 1. X-ray tomographies of a flax fibres cross-section

## II. MATERIALS AND METHODS

### A. The microrobotic tensile test machine and the different grippers

Figure 2 shows the principle of the microrobotic tensile test machine that has been developed at Tampere University. The right jaw is the tested gripper that holds one end of the fibre tested. The type of actuator B, used to open and close the gripper, varies depending on the gripper being tested (Figure 2 c and d). Linear actuators D and E and rotary actuator F allow the fibre to be aligned with the  $+\vec{x}$  tensile axis. The other end of the fibre is clamped by compression in the left jaw. The left jaw is screwed to actuator A which is not operated to open or close the jaw. Force sensor G (Futek LSB200, measuring range: 0 g-100 g) is positioned between the framework and actuators A and H. During the

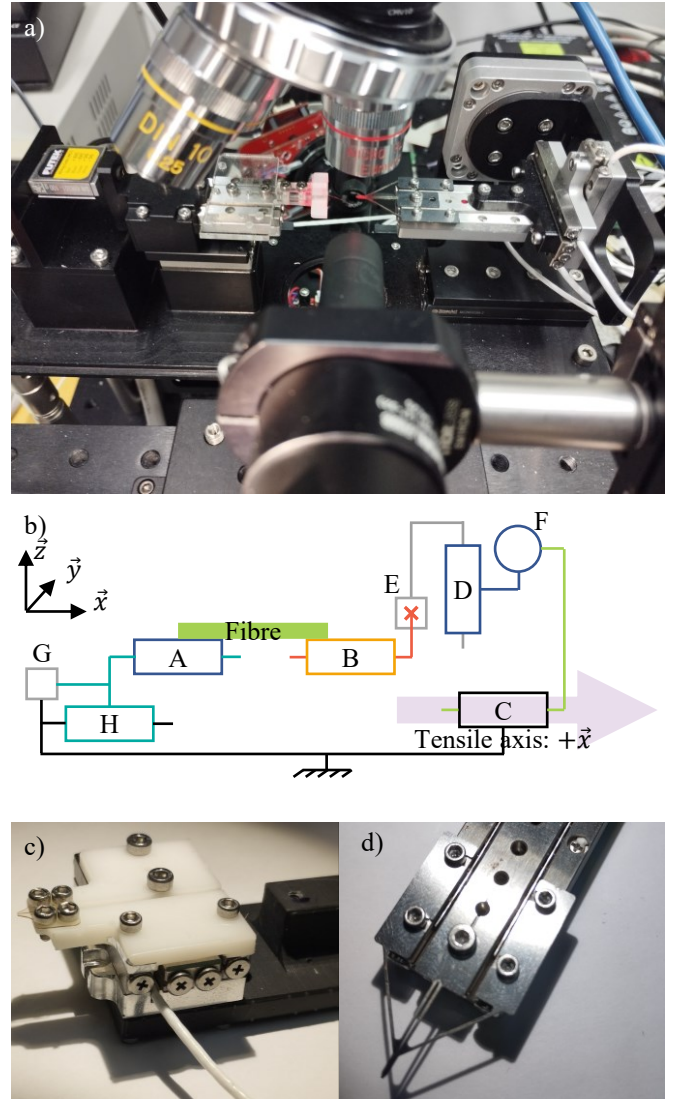


Fig. 2. a) The microrobotic tensile test machine b) kinematic diagram of the tensile test machine and close view of the microrobotic grippers c) Crocodile Gripper (CG-SU8 polymer) and d) Wave Gripper (WG-stainless steel)

tensile test, actuator A is fixed in relation to actuator H and the translation of actuator B in relation to the framework is given by actuator C. Actuators E, D and F are not actuated during the tensile test.

Two optical microscopes equipped with cameras are used to observe the test, one along the  $\vec{z}$  axis, called top view, and the other along the  $\vec{y}$  axis, called side view. Image acquisition frequencies are respectively 40 fps for the side view and 24 fps for the top view.

Figure 3 compares the two types of gripping systems with a flat surface finger gripper (Figure 3 a), commercially available (SmarAct GmbH, Oldenburg, Germany). The first type of gripper (Figure 3 b), designed by Tampere University and manufactured by SmarAct GmbH, is called a Wave Gripper (WG) because the parts that hold the fibre are shaped like two sinusoids that interlock when closed. It is made of

stainless steel. It is screwed onto a SmarAct actuator (SLC-1740), which is actuator B (Figure 2 d). The central part of actuator B slides in relation to the lateral parts. When the central part of the actuator moves in one direction, the gripper opens and closes when the actuator moves in the opposite direction. The first point of contact between the two parts holding the fibre is at the tip of the gripper when it closes. They then gradually come into contact along their entire working length. When they are in contact, the tip of the gripper reopens slightly.

The second type of gripper (Figure 3 c) is called a Crocodile Gripper (CG) because the two parts that hold the fibre are shaped like triangular teeth that indent the fibre. They are made of 200  $\mu\text{m}$  thick layer of SU-8 3050 transparent photoresistive epoxy (Kayaku Advanced Materials). They are fabricated on a silicon wafer that is coated with an aluminium sacrificial layer, using standard photolithography techniques, and released via etching process [21]. It is designed and manufactured by Tampere University. It is screwed onto a SmarAct actuator (SLC-1730) that takes the place of actuator B (Figure 2 c). The actuator opens and closes the gripper by translating one of the parts while the other remains fixed. When the gripper closes, the first point of contact is at the tip of the gripper, and as the gripper deforms, the contact spreads to the other indentation teeth.

For each gripper, before a series of tensile tests, the left jaw and the gripper are brought into contact in order to visually adjust their position in the  $(\vec{x}, \vec{z})$  plane using the side view camera and  $(\vec{x}, \vec{y})$  plane by naked eye.

### B. Test conditions and identification of mechanical properties

Fifty single individual flax fibres from FlaxTape™ (EcoTechnilin SAS, Valliquerville, France) are isolated and both ends of each are glued onto a paper frame. The gauge length of the tested fibre is approximately 10 mm. An optical microscope (Nikon Eclipse LV150) is used to verify that the flax fibre is a single fibre, with a relatively consistent cross-section along its entire length and free from defects such as kink bands [11]. To easier manipulate the fibre during the following operations, it is glued on a paper frame. One end of the fibre is cut from the paper frame along with the two adjacent sides of the frame. The remaining end of the fibre on the paper frame is clamped onto the left jaw between two surfaces, one made of acrylic and the other made of acrylic but covered with PDMS. The gripper is opened and cleaned with a small brush. The left jaw is then screwed onto actuator A (Figure 2 b) of the tensile test machine. The free end of the fibre is grasped with the gripper, trying to have the same length (approximately 700  $\mu\text{m}$ ) of fibre gripped inside the gripper in all cases (flat, WG, CG). For both grippers, the clamping force level is experimentally determined to avoid failure of the fibre in the gripper by trial and error tests; it is then set to the same actuator position for all the tensile tests.

The tensile test is performed with a displacement speed of 16  $\mu\text{m s}^{-1}$ , recording force, displacement of the actuator C

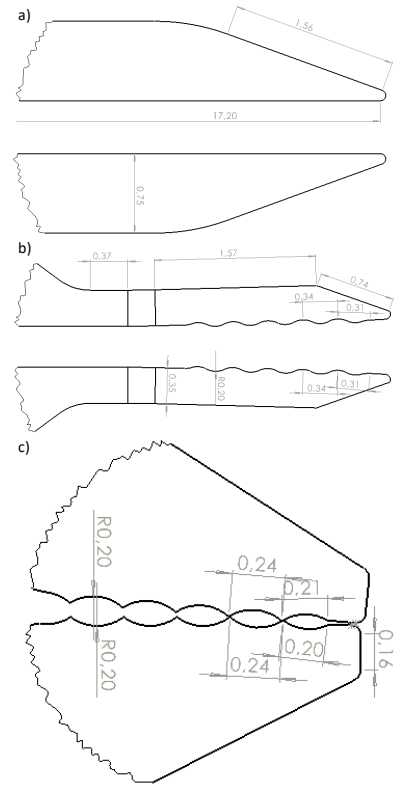


Fig. 3. Drawing (unit millimetre) of a) Flat surface finger gripper b) Wave Gripper (WG-stainless steel) c) Crocodile Gripper (CG-SU8 polymer)

(Figure 2) and both top and side camera images. When the fibre breaks, if it is possible, the free end of the fibre that has just broken is glued onto a piece of paper in order to observe it under a microscope. Ten fibres per type of gripper are tested (WG and CG). The remaining fibres were employed for training to the use of the tensile test machine and fine-tuning the experimental protocol.

Following the tensile test, the remaining part or parts of the fibre are observed under a digital microscope (Keyence VHX-5000). Assuming the cross-section of the fibres is circular, their diameters are measured in three zones (Figure 4), each distributed approximately evenly along the initial length of the fibre.

- zone 1 is always joined to the left jaw
- zone 3 is always in the compressed region in the gripper

In case of failure:

- zone 2 is positioned in the centre of the left part of the fibre clamped to the left jaw

Notice that the positions of those zones depend on the location of the failure point. For some fibres, it may not be feasible to measure in certain zones due to the remaining part being too small to be collected after failure.

In case of slippage, zone 2 is in the middle of the fibre.

To work out the stress ( $\sigma = \frac{F}{A}$  where  $F$  is the recorded force and  $A$  the area of the cross-section of the fibre), the average of the diameters measured in zones 1 and 2 is

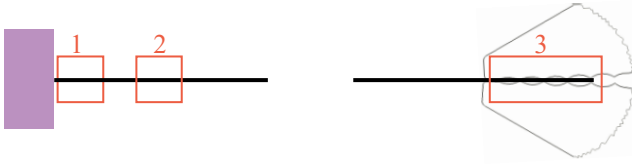


Fig. 4. Zones of measurement of the diameter of the fibre cross-section after a tensile test

used. If measurements in zones 1 and 2 are unavailable, the diameter measured in another zone is used. The strain ( $\epsilon = \frac{\Delta L}{L}$  where  $\Delta L$  is the change in fibre gauge length and  $L$  the initial gauge length of the fibre) is derived from the displacement measured without compliance correction, considering the initial length of the fibre as 10 mm. Young's modulus is determined within the strain range of 0.15 % to 0.35 %.

### III. RESULTS AND DISCUSSION

Several events can occur during a tensile test. The fibre can break at different points such as in its gauge section or close to the clamps. The gauge section is defined as the section that is not contiguous to the jaw nor to the gripper (Figure 5).

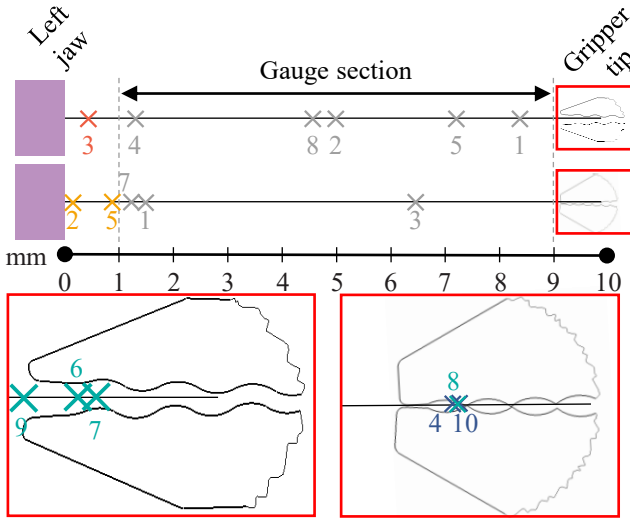


Fig. 5. Approximated failure point and zone at which this point is located

For the tensile tests carried out for this study, the gauge section corresponds to the eight millimetres in the centre of the fibre (one millimetre discarded at each end). According to the standard [22], a test is valid when the fibre breaks in the gauge section. Longitudinal Young's modulus and stress at failure are therefore identified for these fibres. Conversely, when the failure is close to the clamp, the test is not considered valid by the standard. In fact, the measured tensile stress is only one component of the possible multiaxial stresses leading to fibre failure. During a tensile test, the fibre can also slip in the jaws. The displacement measured in this case is not a displacement

that produces a tensile force on the fibre. However, only the displacement producing a tensile force on the fibre is included in the calculation of the strain [23]. According to the standard, this test should therefore be discarded.

The frequency of each scenario, i.e. the characteristic test events observed during ten tensile tests for each gripper (slippage and/or failure of the fibre at a given location), is shown in Figure 6 a. These observations are made possible by the two microscopes installed on the tensile test machine. Primarily, the incidence of slip-free tests is notably higher with these grippers compared to flat finger ones, as the latter consistently experienced some level of slippage making it impossible to use them as gripping jaws in a tensile test. Among the ten fibres tested with each gripper, respectively five for the WG and three for the CG broke in the gauge section. The results obtained with the WG therefore appear more promising.

Throughout the tests, the temperature was  $22.2 \pm 0.7^\circ\text{C}$  and the relative humidity in the room was  $21.6 \pm 3.5\%$ . The force/displacement curves are drawn in Figure 6 b and c. Each curve is color-coded, based on the zone where the failure point is observed and the scenario witnessed during the test. For some curves, a sudden decrease (not leading to a zero force) in the measured tensile force is observed. This corresponds to the slippage of the fibre within the gripper. The Young's modulus of each fibre tested is identified from its force/displacement curve and from the diameter measurements taken after testing, i.e. for an elastic behaviour, the longitudinal Young's modulus  $E$  is the slope of the stress/strain curve ( $\sigma = E\epsilon$ ). For all tested fibres, the longitudinal Young's modulus can be determined within the range 0.15 % and 0.35 % of strain, as slippage only occurs outside this range. The stress at failure is identified for the scenarios where the fibre fails in the gauge section. When the fibre slips into the grippers during the test and does not break, the maximum stress measured is a lower bound of the stress at failure. The same applies if the fibre first slips into the grippers and then breaks as well as when the fibre breaks in the left jaw or at the gripper tip.

Table I shows the values of Young's moduli and stresses at failure identified for the fibres tested with each gripper. These values are in line with the literature: the flax fibre Young's modulus is in the range of  $46.9 \pm 15.7\text{ GPa}$  to  $68.2 \pm 35.8\text{ GPa}$  and its stress at failure is in the range of  $850 \pm 359\text{ MPa}$  [11]. However, care must be taken with the cross-sectional measurement of the fibre retained [24], notably three fibres with a higher Young's modulus and/or stress at failure are, for this reason, considered as outliers. This validates the concept of using grippers with a specific geometry to direct grip the flax fibres during a tensile test. Nonetheless, the fibre often slips in the gripper: for instance two fibres out of ten for the WG and four out of ten for the CG. Only one parameter influencing this scenario could be fully identified experimentally. It is observed on the force/displacement curves (Figure 6 b and c) that with both grippers tested, excessive tensile force leads to slippage.

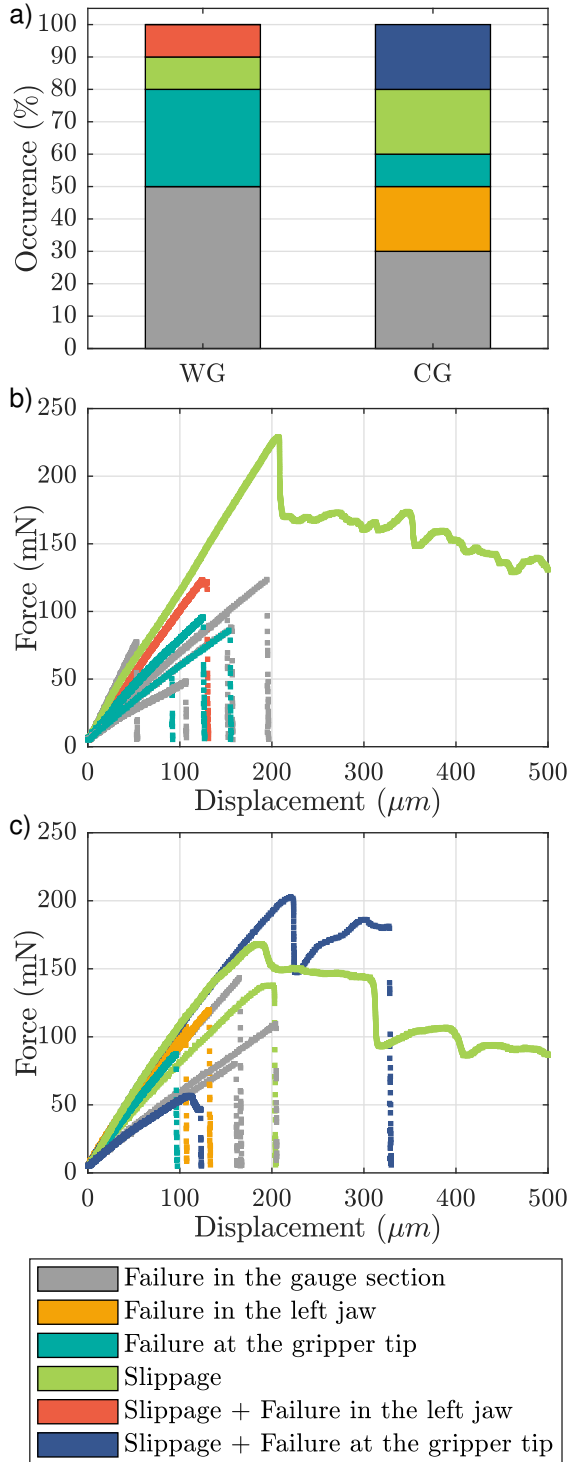


Fig. 6. a) The different scenarios emerging during tensile tests on ten flax fibres per type of gripper & force/displacement curves obtained with b) WG and c) CG

TABLE I  
THE IDENTIFIED YOUNG'S MODULUS ( $E_L$ ) AND STRESS AT FAILURE ( $\sigma_f$ ) (\* OUTLIERS NOT CONSIDERED – \*\* IMPOSSIBLE TO MEASURE THE DIAMETER – \*\*\* ONLY CONSIDERING FAILURE IN THE GAUGE SECTION)

WG			
Fibre no.	Scenario	$E_L$ GPa	$\sigma_f$ MPa
1	Failure in the gauge section	66.0	1 013
2	Failure in the gauge section	26.3	403
3	Slippage + Failure in the left jaw	58.5	$\geq 704$
4*	Failure in the gauge section	203.4	1 119
5	Failure in the gauge section	24.7	431
6 **	Failure at the gripper tip		
7*	Slippage	141.0	$\geq 2 527$
8	Failure at the gripper tip	35.1	423
9	Failure in the gauge section	13.8	144
10	Failure at the gripper tip	57.0	828
		$40.2 \pm 20.2$	$622 \pm 422$ ***
CG			
1	Failure in the gauge section	67.3	1 007
2 *	Failure in the left jaw	116.5	1 220
3	Failure in the gauge section	72.9	1 100
4	Slippage + Failure at the gripper tip	27.4	$\geq 500$
5	Failure in the left jaw	42.6	500
6	Slippage	39.2	$\geq 640$
7	Failure in the gauge section	37.5	720
8	Failure at the gripper tip	54.6	510
9	Slippage	30.4	440
10	Slippage + Failure at the gripper tip	17.2	$\geq 180$
		$43.2 \pm 18.5$	$942 \pm 198$ ***

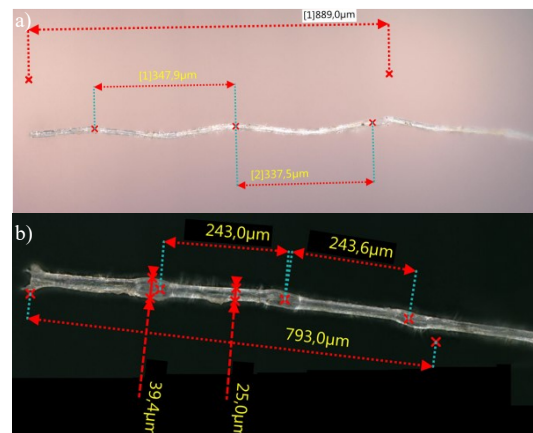


Fig. 7. Rest of fibres in the grasping zone tested a) with the WG and b) with the CG

Specifically, slippage occurs at approximately 130 mN for the WG and approximately 168 mN for the CG.

Figure 7 shows microscope images, after a tensile test, of the fibre region clamped into the gripper. For the WG type, the part of the fibre clamped in the gripper is shaped like the same wave as the gripper and appears to be irreversibly deformed (Figure 7 a). In the case of the CG, the damaged areas are at the indentation points, where a shear stress appears. That results in local flattening of the fibre (Figure 7 b). Consequently, these fibre deformations could be the cause of failures at the gripper tip. The shape of the grippers, especially the WG, has a good potential for tensile testing but could be improved in future works, for example by increasing the coefficient of friction between the fibre and the finger gripper or by controlling the clamping force of the fibre in the grippers.

## IV. CONCLUSIONS

The aim of this article is to investigate the potential benefits of using a microrobotic approach to carry out tensile tests on plant fibres, which are particularly small (diameter in the order of 20  $\mu\text{m}$ ). To this purpose, an experimental microrobotic platform has been developed at Tampere University (Finland). It is equipped with micro-grippers for clamping the fibre and then carrying out tensile tests. As a fibre always slips from a flat finger gripper, two specific forms of gripper have been studied to ensure good control of fibre embedding conditions during the tests. A series of ten tensile tests for each type of gripper was successfully carried out. All these tests proved to be workable, enabling us to identify the longitudinal Young's modulus and the stress at failure. The values obtained are in line with the data available in the literature, enabling to validate the potential of this microrobotic approach. This approach also seems relevant for the mechanical characterisation of synthetic fibres such as carbon, glass as well as hair for the cosmetics industry.

These results appear disruptive with currently available methods, as they enable to envision significant facilitation of the entire process, from fibre preparation to testing and data analysis. Also, these tests can be largely automated, making it possible to carry out much larger and statistically richer test campaigns. This new approach to robotic automation will also resolve known statistical biases for which no solution is found yet.

## ACKNOWLEDGMENTS

This work is supported by the Région Bourgogne Franche-Comté, the FEMTO-ST scientific board for the student ambassador award as well as the Université de Franche-Comté for the "Mobilité Internationale des Doctorants" grant. This work has been partially funded by the DYNABOT Project (ANR-21-CE10-0016), the EIPHI Graduate School (ANR-17-EURE-0002) and the French RENATECH and ROBOTEX networks (TIRREX ANR-21-ESRE-0015) through their FEMTO-ST technological facilities MIMENTO, MIFHySTO and CMNR.

The research leading to these developments has received funding from the European Union's Horizon 2020 research and innovation programme under the Marie Skłodowska-Curie grant agreement No 764713 (FibreNet), and from the doctoral education programme of Faculty of Medicine and Health Technology at Tampere University. We also acknowledge Fibrobotics Co. for designing the hardware platform.

## REFERENCES

- [1] A. Bourmaud *et al.*, "Towards the design of high-performance plant fibre composites," *Progress in Materials Science*, vol. 97, pp. 347–408, 2018.
- [2] K. L. Pickering, M. A. Efeudy, and T. M. Le, "A review of recent developments in natural fibre composites and their mechanical performance," *Composites Part A: Applied Science and Manufacturing*, vol. 83, pp. 98–112, 2016.
- [3] M. Ramesh, "Flax (*linum usitatissimum* L.) fibre reinforced polymer composite materials: A review on preparation, properties and prospects," *Progress in Materials Science*, vol. 102, pp. 109–166, 2019.
- [4] S. Chokshi, V. Parmar, P. Gohil, and V. Chaudhary, "Chemical composition and mechanical properties of natural fibers," *Journal of Natural Fibers*, vol. 19, no. 10, pp. 3942–3953, 2022.
- [5] A. N. André *et al.*, "Automating robotic micro-assembly of fluidic chips and single fiber compression tests based on xytheta visual measurement with high-precision fiducial markers," *IEEE Trans. on Automation Science and Engineering*, 2022.
- [6] J. Govilas *et al.*, "Platen parallelism significance and control in single fiber transverse compression tests," *Composites Part A: Applied Science and Manufacturing*, vol. 159, p. 106990, 2022.
- [7] M. Žižek, C. Czubala, and U. Hirn, "How the test setup can affect single fiber tensile testing," *Journal of Natural Fibers*, vol. 21, no. 1, p. 2328264, 2024.
- [8] F. Mesquita, S. Bucknell, Y. Leray, S. V. Lomov, and Y. Swolfs, "Single carbon and glass fibre properties characterised using large data sets obtained through automated single fibre tensile testing," *Composites Part A: Applied Science and Manufacturing*, vol. 145, p. 106389, 2021.
- [9] D. Ren, Z. Yu, W. Li, H. Wang, and Y. Yu, "The effect of ages on the tensile mechanical properties of elementary fibers extracted from two sympodial bamboo species," *Industrial Crops and Products*, vol. 62, pp. 94–99, 2014.
- [10] S. Amroune, A. Belaadi, M. Bouchak, A. Makhlof, and H. Satha, "Statistical and experimental analysis of the mechanical properties of flax fibers," *J. of Natural Fibers*, vol. 19, no. 4, pp. 1387–1401, 2022.
- [11] E. Richely *et al.*, "A critical review of the ultrastructure, mechanics and modelling of flax fibres and their defects," *Progress in Materials Science*, vol. 124, p. 100851, 2022.
- [12] S. Joannès, F. Islam, and L. Laiarinandrasana, "Uncertainty in fibre strength characterisation due to uncertainty in measurement and sampling randomness," *Applied Composite Materials*, vol. 27, pp. 165–184, 2020.
- [13] R. Ganesh, A. A. Obaid, and J. W. Gillespie Jr, "Experimental determination of bimodal strength distribution of s-glass fibers," *Composites Part B: Engineering*, vol. 254, p. 110559, 2023.
- [14] L. C. Pardini and L. G. B. Manhani, "Influence of the testing gage length on the strength, young's modulus and weibull modulus of carbon fibres and glass fibres," *Materials research*, vol. 5, pp. 411–420, 2002.
- [15] S. Yao, X. Zhang, B. Zhu, H. Li, L. Yu, and S. Fatikow, "A microvision-based motion measurement system for nanopositioners using the feature-to-phase method," *IEEE Transactions on Instrumentation and Measurement*, vol. 72, pp. 1–11, 2023.
- [16] G. Adam *et al.*, "An overview of microrobotic systems for microforce sensing," *Annual Review of Cont., Rob., and Auton. Syst.*, vol. 7, 2024.
- [17] B. Komati *et al.*, "Automated robotic microassembly of flexible optical components," in *Int. Symp. on Ass. and Manuf.*, 2016, pp. 93–98.
- [18] R. Hannouch *et al.*, "Robotic-based selection, manipulation and characterization of 3d microscale particles with complex structures in sem," in *Int. Conf. on Manip. Autom. and Rob. at Small Scales*. IEEE, 2023.
- [19] B. Tiwari, M. Ghorbani, D. Cisier, and Y. Perriard, "Towards development of a novel variable stiffness instrumented gripper," in *Int. Conf. on Control, Mechatronics and Automation*. IEEE, 2023, pp. 392–396.
- [20] P. Saketi, S. K. Latifi, J. Hirvonen, S. Rajala, A. Vehkaoja, T. Salpavaara, J. Leikkala, and P. Kallio, "Pvdf microforce sensor for the measurement of z-directional strength in paper fiber bonds," *Sensors and Actuators A: Physical*, vol. 222, pp. 194–203, 2015.
- [21] T. Salpavaara, T. Joki, A. Skogberg, M. Calejo, J. Leikkala, S. Narkilahti, and P. Kallio, "Microfabricated porous su-8 membranes as innervation interfaces for hipsc-neurons in microfluidic devices," *Journal of Physics Communications*, vol. 5, no. 11, p. 115003, 2021.
- [22] "Fibres de renfort Fibres de lin pour composites plastiques Partie 2 : Détermination des propriétés en traction des fibres élémentaires," Association Française de Normalisation (AFNOR), Standard NF T25-501-2, Mar. 2015.
- [23] A. E. Engelbrecht-Wiggans and A. L. Forster, "Analysis of strain correction procedures for single fiber tensile testing," *Composites Part A: Applied Science and Manufacturing*, vol. 167, p. 107411, 2023.
- [24] M. Aslan, G. Chinga-Carrasco, B. F. Sørensen, and B. Madsen, "Strength variability of single flax fibres," *Journal of materials science*, vol. 46, pp. 6344–6354, 2011.